Celestial Mechanics and Dynamical Astronomy (2018) 130:48
https://doi.org/10.1007/s10569-018-9841-9

ORIGINAL ARTICLE

Symmetries and choreographies in families that bifurcate from the polygonal relative equilibrium of the *n*-body problem

Renato Calleja[1] · Eusebius Doedel[2] · Carlos García-Azpeitia[3]

Received: 3 April 2017 / Revised: 22 March 2018 / Accepted: 7 June 2018 / Published online: 6 July 2018

Abstract
We use numerical continuation and bifurcation techniques in a boundary value setting to follow Lyapunov families of periodic orbits and subsequently bifurcating families. The Lyapunov families arise from the polygonal equilibrium of n bodies in a rotating frame of reference. When the frequency of a Lyapunov orbit and the frequency of the rotating frame have a rational relationship, then the orbit is also periodic in the inertial frame. We prove that a dense set of Lyapunov orbits, with frequencies satisfying a diophantine equation, correspond to choreographies. We present a sample of the many choreographies that we have determined numerically along the Lyapunov families and along bifurcating families, namely for the cases $n = 3$, 4, and 6–9. We also present numerical results for the case where there is a central body that affects the choreography, but that does not participate in it. Animations of the families and the choreographies can be seen at the link below.

1 Introduction

The study of n equal masses that follow the same path has attracted much attention in recent years. The first solution that differs from the classical Lagrange circular orbit was discovered numerically by Moore (1993), where three bodies follow one another around the now famous Figure-Eight orbit. This orbit was located by minimizing the action among symmetric paths.

http://mym.iimas.unam.mx/renato/choreographies/index.html.

✉ Renato Calleja
calleja@mym.iimas.unam.mx

Eusebius Doedel
doedel@cs.concordia.ca

Carlos García-Azpeitia
cgazpe@ciencias.unam.mx

1 Instituto de Investigaciones en Matemáticas Aplicadas y en Sistemas, Universidad Nacional Autónoma de México, Mexico, Mexico

2 Department of Computer Science, Concordia University, Montreal, Canada

3 Facultad de Ciencias, Universidad Nacional Autónoma de México, Mexico, Mexico

Independently Chenciner and Montgomery (2000) gave a rigorous mathematical proof of the existence of this orbit, by minimizing the action over paths that connect a colinear and an isosceles configuration. Such solutions are now commonly known as "choreographies," after the work in Simó (2001), Simó presented extensive numerical computations of choreographies for many choices of the number of bodies.

The results in Chenciner and Montgomery (2000) mark the beginning of the development of variational methods, where the existence of choreographies can be associated with the problem of finding critical points of the classical action of Newton's equations of motion. The main obstacles encountered in the application of the principle of least action are the existence of paths with collisions and the lack of compactness of the action. Ferrario and Terracini (2004) applied the principle of least action systematically over symmetric paths to avoid collisions, using ideas introduced by Marchal (2002). For the action in a rotating frame, it is shown in Barutello and Terracini (2004) that, depending on the frequency of rotation, there is no minimizer, or the n-polygon is a minimizer, or different choreographies are minimizers. For a discussion of these and other variational approaches, we refer to Barutello et al. (2008), Chen (2003), Ferrario (2006), Ferrario and Portaluri (2008), Terracini and Venturelli (2007), and the references therein.

Chenciner and Féjoz (2009) pointed out that choreographies appear in dense sets along Vertical Lyapunov families that arise from n bodies rotating in a polygon; see also Chenciner et al. (2005). In Chenciner and Féjoz (2009), the existence of the Vertical Lyapunov families is proved using the Weinstein–Moser theory. A fact established in Chenciner and Féjoz (2009), for orbits close to the polygonal equilibrium with $n \leq 6$, is that when the frequency varies along the Vertical Lyapunov families, then an infinite number of choreographies exists. While similar computations can be carried out for other values of n, there is no general analytical proof for all n.

Theorems 30 and 38 in García-Azpeitia and Ize (2013) prove the existence of Planar and Vertical Lyapunov families using equivariant degree theory. The norm or the period of the orbits along a family tends to infinity, or the family ends in a collision, or otherwise it returns to other trivial solutions (equilibria). Similar bifurcation theorems have been proved for the restricted body problem in García-Azpeitia and Ize (2011a, b). Numerical computations in Calleja et al. (2016) show that each of the families ends in a collision orbit, goes to infinity in Sobolev norm, has unbounded period, returns to other equilibria, or exhibits a mix of these alternatives.

The purpose of our current work is to use advanced computational methods to determine the families and subsequently bifurcating families of the n body problem and to locate choreographies along such families in a systematic fashion. To explain our numerical results, we first recall some relevant results from García-Azpeitia and Ize (2013). Let $(q_j(t), z_j(t)) \in \mathbb{C} \times \mathbb{R}$ be the position of the jth body in space at time t. Then, $(u_j, z_j) \in \mathbb{C} \times \mathbb{R}$ are the positions of the bodies in a rotating frame, with $q_j(t) = e^{i\omega t} u_j(t)$. The equations of motion of n bodies of unit mass in this rotating frame are given by

$$\begin{aligned} \ddot{u}_j + 2\omega\, i\, \dot{u}_j &= \omega^2 u_j - \sum_{j'=1(j'\neq j)}^{n} \frac{u_j - u_{j'}}{\left\|(u_j, z_j) - (u_{j'}, z_{j'})\right\|^3}, \\ \ddot{z}_j &= -\sum_{j'=1(j'\neq j)}^{n} \frac{z_j - z_{j'}}{\left\|(u_j, z_j) - (u_{j'}, z_{j'})\right\|^3}. \end{aligned} \tag{1}$$

The polygonal relative equilibrium consists of the positions

$$u_j = e^{ij\zeta}, \quad z_j = 0, \quad \zeta = \frac{2\pi}{n}, \tag{2}$$

which is an equilibrium of (1) when the frequency is fixed to be $\omega = \sqrt{s_1}$, where $s_1 = \frac{1}{4}\sum_{j=1}^{n-1} \frac{1}{sin(j\zeta/2)}$.

The emanating Lyapunov families have starting frequencies that are equal to the normal frequencies of oscillation of equilibrium (2). To be precise, let ν be the frequency of the Lyapunov orbit (u_j, z_j), *i.e.*, the period is $T = 2\pi/\nu$. Then,

$$w_j(t) = u_j(t/\nu), \quad \xi_j(t) = z_j(t/\nu),$$

are renormalized 2π-periodic functions. The theorem in García-Azpeitia and Ize (2013) states that for $n \geq 6$ and for each integer k such that

$$3 \leq k \leq n-3,$$

the polygonal relative equilibrium has one *family of planar periodic solutions* with symmetries

$$w_j(t) = e^{ij\zeta} w_n(t + jk\zeta). \tag{3}$$

The proof in García-Azpeitia and Ize (2013) predicts solutions with $k = 2$ or $n-2$ if the linear equations at the polygonal equilibrium have normal modes corresponding to these symmetries. In fact, three cases occur for different values of n: for $n = 4, 5, 6$, there are no solutions with $k = 2$ or $n-2$; for $n = 7, 8, 9$, there are two solutions with $k = 2$ and no solutions with $k = n-2$; and for $n \geq 10$, there is one solution with $k = 2$ and one with $k = n-2$.

In the case of spatial Lyapunov families, the eigenvalues of the linearized system of equations are given explicitly by $i\sqrt{s_k}$ with

$$s_k = \frac{1}{4}\sum_{j=1}^{n-1} \frac{\sin^2(kj\zeta/2)}{\sin^3(j\zeta/2)}, \tag{4}$$

for $k = 1, \ldots, n-1$; see Chenciner and Féjoz (2009) and García-Azpeitia and Ize (2013). The eigenvalues $i\sqrt{s_k}$ are resonant due to the fact that $s_{n-k} = s_k$ for $1 \leq k < n/2$. Moreover, the first eigenvalue $i\sqrt{s_1}$ is resonant with the triple planar eigenvalue $i\sqrt{s_1}$ and hence is highly degenerate. These resonances can be dealt with using equivariant degree theory in Ize and Vignoli (2003). The theorem in García-Azpeitia and Ize (2013) states that for $n \geq 3$ and for each k such that

$$1 \leq k \leq n/2,$$

the polygonal relative equilibrium has one *family of spatial periodic solutions* which start with frequency $\nu = \sqrt{s_k}$, have symmetries (3),

$$\xi_j(t) = \xi_n(t + jk\zeta), \tag{5}$$

and

$$w_n(t) = w_n(t + \pi), \quad \xi_n(t) = -\xi_n(t + \pi). \tag{6}$$

For example, for the case where $k = n/2$ and n is even, we have $k\zeta = \pi$. Then, symmetries (3), (5) and (6) imply that

$$w_j(t) = e^{ij\zeta} w_n(t + j\pi) = e^{ij\zeta} w_n(t),$$

$$\xi_j(t) = \xi_n(t + jk\zeta) = (-1)^j \xi_n(t).$$

Solutions having these symmetries are known as Hip-Hop orbits and have been studied in Barrabés et al. (2006). Solutions with symmetries (3) and (5) are "traveling waves" in the sense that each body follows the same path, but with a rotation and a time shift. The symmetries allow us to establish that a dense set of solutions along the family are choreographies in the inertial frame of reference.

We say that a Planar or Spatial Lyapunov orbit is $\ell : m$ *resonant* if its period and frequency are

$$T = \frac{2\pi}{\sqrt{s_1}} \left(\frac{\ell}{m} \right), \quad \nu = \sqrt{s_1}\, \frac{m}{\ell},$$

where ℓ and m are relatively prime, and such that

$$k\ell - m \in n\mathbb{Z}.$$

In Theorem 1, we prove that $\ell : m$ resonant Lyapunov orbits are choreographies in the inertial frame. Each of the integers k, ℓ, and m plays a different role in the classification of the choreographies. Indeed, the projection of the choreography onto the xy-plane has winding number ℓ around a center and is symmetric with respect to the $\mathbb{Z}_m$-group of rotations by $2\pi/m$. In addition, the n bodies form groups of d-polygons, where d is the greatest common divisor of k and n. Some choreographies wind around a toroidal manifold with winding numbers ℓ and m, i.e., the choreography path is an (ℓ, m)-torus knot. In particular, such orbits appear in families that we refer to as "Axial families," e.g., in Fig. 7. We note that for other values of ℓ and m the orbits of the n bodies in the inertial frame are also closed, but consist of multiple curves, called "*multiple choreographic solutions*" in Chen (2003).

We use robust and highly accurate boundary value techniques with adaptive meshes to continue the Lyapunov families. An extensive collection of python scripts that reproduce the results reported in this article for a selection of values of n will be made freely available. These scripts control the software AUTO to carry out the necessary sequences of computations. One advantage of the continuation approach is that this procedure can be implemented for other equations with similar symmetries, e.g., this approach to the computation of choreographies can be extended to the n-vortex problem, to a periodic lattice of Schrödinger sites, and to the n-body problem with Lennard-Jones or other integrable potential. In Chenciner and Féjoz (2009), the numerical continuation of the Vertical Lyapunov families is implemented as local minimizers in subspaces of symmetric paths. Presumably, not all families are local minimizers restricted to subspaces. Our procedure allows the numerical continuation of all Planar and all Vertical Lyapunov families that arise from simple eigenvalues and some families that arise from double eigenvalues. The systematic computation of periodic orbits that arise from eigenvalues of higher multiplicity remains under investigation. Computer-assisted proofs of the existence of choreographies have been given in, for example, Kapela and Zgliczynski (2003) and Kapela and Simó (2007, 2017). Such techniques can validate our numerical computations, to prove the existence of the dense sets of choreographies presented in our article.

Previous numerical work has explored the existence of many choreographies as minimizers of the action; see, for example, Barutello and Terracini (2004), Chen (2003), Chenciner et al. (2002), Montaldi and Steckles (2013) and Simó (2001). The choreographies obtained in these papers have many similarities with solutions that we obtain by continuation methods. However, it is not easy to establish a systematic relation between the minimizers of the action and solutions along continuation families. For instance, one of the main goals in Chenciner

and Féjoz (2009) is to give evidence of a connection via families of periodic solutions between the triangle and a Figure-Eight choreography of Marchal, which is a minimizer of the action. This remains an open problem. However, we do present an analogous connection for the case of seven bodies, where the heptagon connects indirectly to a Figure-Eight choreography, namely via a Vertical Lyapunov family with $k = 2$ and an Axial family that bifurcates from the Vertical family. The Figure-Eight choreography then corresponds to a 1:2-resonant orbit along this Axial family. Although the Figure-Eight orbit discovered by Moore is still the only choreography that has been proved to be stable Kapela and Simó (2007), we have found strong evidence of other stable choreographies.

The classification of the choreographies by numbers k, ℓ, and m appears in a natural manner in our continuation method. In Barutello and Terracini (2004) and Montaldi and Steckles (2013), other classifications that are more natural for variational methods are used for planar choreographies. The classification in Barutello and Terracini (2004) holds for three bodies in shape space, while Montaldi and Steckles (2013) contains a classification for an arbitrary number of bodies. Many connected components of loop space exist for a given symmetry class in Montaldi and Steckles (2013). There is a choreography minimizer for the case of strong potentials in each connected component. It is an open problem whether there is a choreography minimizer for the Newton potential in every component. Therefore, our approach presents complementary information in the classification of choreographies with respect to previous classifications.

In Sect. 2, we prove that a dense set of orbits along the Lyapunov families correspond to choreographies. In Sect. 3, we describe the numerical continuation procedure used to determine the periodic solution families, and in Sect. 4, we give examples of numerically computed Lyapunov families and some of their bifurcating families. In Sect. 5, we provide a sample of the choreographies that appear along Planar Lyapunov families. Section 6 presents choreographies along the Vertical Lyapunov families and along some of their bifurcating families. In particular, a family of axially symmetric orbits forms a connection between a Vertical family and a Planar family. Choreographies along such tertiary Planar families are referred to as "unchained polygons" in Chenciner and Féjoz (2009).

In Sect. 7, we present results of the numerical continuation of a Planar family, starting from the 3-body Figure-Eight choreography. Along this family, we locate other choreographies of interest. In Sect. 7, we also determine families that arise from the Maxwell relative equilibrium, i.e., with an additional body added at the center of the n-polygon. This configuration has been used as a model to study the stability of the rings of Saturn, as established in Moeckel (1994) and in García-Azpeitia and Ize (2013), Vanderbei and Kolemen (2007), and Roberts (2000) for $n \geq 7$. Using a similar approach as in the earlier sections, we determine solutions where n bodies of equal mass 1 follow a single trajectory, but with an additional body of mass μ at or near the center. While this extra body does not participate in the choreography, it does affect its structure and its stability properties.

2 Choreographies and Lyapunov families

Let $x_j = (w_j, \xi_j)$, $x = (x_1, \ldots, x_n)$, and let $\Psi = \{x \in \mathbb{R}^{3n} : x_i = x_j\}$ be the collision set, when two or more of the bodies collide, and let $H^2_{2\pi}(\mathbb{R}^{3n} \backslash \Psi)$ be the open subset of the Sobolev space $H^2(\mathbb{R}^{3n})$ consisting of the collision-free periodic (and continuous) functions. We define the set of parameters $\Lambda = \{\nu > 0\}$ and the space of zero z-average functions

$x(t) \in \mathbb{R}^{3n}$,

$$X = \{x \in L^2_{2\pi}(\mathbb{R}^{3n}) : \sum_{j=1}^{n} \int_0^{2\pi} \xi_j \, \mathrm{d}t = 0\}.$$

Define the operator

$$f : X \cap H^2_{2\pi}(\mathbb{R}^{3n} \backslash \Psi) \times \Lambda \to X$$

as $f(x; \nu) = (f_1, \ldots, f_n)$ with components given by

$$f_j(x) = \begin{pmatrix} -\nu^2 \ddot{w}_j - 2\nu\sqrt{s_1}\, i\, \dot{w}_j - V_{w_j} \\ -\nu^2 \ddot{\xi}_j - V_{\xi_j} \end{pmatrix},$$

where the amended potential is

$$V(x) = \frac{1}{2} \sum_j \|w_j\|^2 + \sum_{j'<j} \frac{1}{\|(w_j, \xi_j) - (w_{j'}, \xi_{j'})\|}.$$

The operator f is well defined in X due to the conservation of momentum in the z-coordinate.

With a change of variables in the Newton equations, the period of (w_j, ξ_j) is fixed at 2π and the frequency ν becomes a bifurcating parameter. Thus, the zeros $(x; \nu)$ of the operator f correspond to $2\pi/\nu$-periodic solutions of the Newton equations of the form

$$q_j(t) = e^{i\sqrt{s_1}t} w_j(\nu t), \qquad z_j(t) = \xi_j(\nu t).$$

In García-Azpeitia and Ize (2013), the global property of the bifurcation of periodic solutions is obtained as a bifurcation of zeros of the Fredholm operator f in the open set $X \cap H^2_{2\pi}(\mathbb{R}^{3n} \backslash \Psi) \times \Lambda$. The analog of the global Rabinowitz theorem in García-Azpeitia and Ize (2013) is that a Lyapunov family forms a continuum $\mathcal{C}$ in $X \cap H^2_{2\pi}(\mathbb{R}^{3n} \backslash \Psi) \times \Lambda$ that is not compact or returns to other bifurcation points (equilibria). The continuum $\mathcal{C}$ is not compact if either the family of periodic solutions (x, ν) ends at an orbit with collisions when $x(t) \to \Psi$, the period goes to infinity when $\nu \to 0$, the Sobolev norm goes to infinity when $|x|_{H^2_{2\pi}} \to \infty$, or the branch goes to an equilibrium when $\nu \to \infty$ (see Alexander and Yorke 1978). Actually, the results in García-Azpeitia and Ize (2013) are obtained for a general polygon with a central mass μ within the context of the Maxwell model for the rings of Saturn. We present a brief description of the numerical computations for $\mu \neq 0$ in Sect. 7.

We rescale time in the Lyapunov orbits to simplify the computations,

$$q_j(t) = e^{it\sqrt{s_1}/\nu} w_j(t), \quad z_j(t) = \xi_j(t), \tag{7}$$

where w_j and ζ_j are 2π-periodic with symmetries (3) and (5). For these orbits, we prove the following:

Lemma 1 *Let*

$$\Omega = \frac{1}{n}\left(k\frac{\sqrt{s_1}}{\nu} - 1\right).$$

Then, a rescaled Planar Lyapunov orbit with frequency ν, given by

$$q_j(t) = e^{i\sqrt{s_1}t/\nu} w_j(t),$$

satisfies

$$q_j(t) = e^{-ij(2\pi)\Omega} q_n(t + jk\zeta).$$

Proof We have

$$q_j(t) = e^{it\sqrt{s_1}/\nu} w_j(t) = e^{it\sqrt{s_1}/\nu} e^{ij\zeta} w_n(t + jk\zeta).$$

Since

$$q_n(t + jk\zeta) = e^{i(t+jk\zeta)\sqrt{s_1}/\nu} w_n(t + jk\zeta),$$

it follows that

$$q_j(t) = e^{it\sqrt{s_1}/\nu} e^{ij\zeta} \left(e^{-i(t+jk\zeta)\sqrt{s_1}/\nu} q_n(t + jk\zeta) \right) = e^{-ij\zeta n\Omega} q_n(t + jk\zeta).$$

□

In particular, if $\Omega \in \mathbb{Z}$, then the Lyapunov solution satisfies

$$q_j(t) = q_n(t + jk\zeta), \tag{8}$$

and is a choreography. In fact, planar choreographies exist for any rational number $\Omega = p/q$ where q is relatively prime to n.

Proposition 1 *If $\Omega = p/q$, with q relatively prime to n, then*

$$q_j(t) = q_n\left(t + jk'\zeta\right), \tag{9}$$

where $k' = q'qk$ with q' the n-modular inverse[1] *of q. Moreover, the solutions $q_n(t)$ is $2\pi m$-periodic, where m and ℓ are relatively prime such that*

$$\frac{\ell}{m} = \frac{np + q}{kq}. \tag{10}$$

Proof If $\Omega = p/q$, the solution satisfies

$$q_j(t) = e^{-i2\pi jp/q} q_n(t + jk\zeta). \tag{11}$$

Since $q'q = 1 + bn$ for some positive number b, we have

$$q_j(t) = q_{j(1+nb)}(t) = e^{-i2\pi jq'p} q_n\left(t + j(q'qk\zeta)\right) = q_n\left(t + jk'\zeta\right). \tag{12}$$

Since

$$\frac{\sqrt{s_1}}{\nu} = \frac{n\Omega + 1}{k} = \frac{np + q}{qk} = \frac{\ell}{m},$$

it follows that $e^{it\sqrt{s_1}/\nu}$ is $2\pi m$-periodic, and since $w_n(t)$ is 2π-periodic, we also have that the function $q_n(t) = e^{it\sqrt{s_1}/\nu} w_n(t)$ is $2\pi m$-periodic. □

Proposition 2 *For $\Omega = p/q$, with q and n relatively prime, the spatial Lyapunov solution is a choreography that satisfies*

$$(q_j, z_j)(t) = (q_n, z_n)\left(t + jk'\zeta\right), \tag{13}$$

where $k' = q'qk$ and $(q_n, z_n)(t)$ is $2\pi m$-periodic.

[1] We say that $q\prime$ is the n-modular inverse of q if $q\prime q$ is congruent to 1 modulus n.

Proof For the planar component of the spatial Lyapunov families, we have $q_j(t) = q_n(t + j(aqk\zeta))$, where $q_n(t)$ is $2\pi m$-periodic. Since $aq = 1 + bn$ and $\zeta = 2\pi/n$, we have in addition that the spatial components satisfy

$$z_j(t) = z_n(t + jk\zeta) = z_n\left(t + jk'\zeta\right),$$

where $z_n(t)$ is 2π-periodic. □

For fixed n, the set of rational numbers p/q such that q and n are relatively prime is dense. If the range of the frequency ν along the Lyapunov family contains an interval, then there is a dense set of rational numbers $\Omega = p/q$ inside that interval. Hence, there is an infinite number of Lyapunov orbits that correspond to choreographies. To be precise, the resonant Lyapunov orbit gives a choreography that has period

$$mT = m\frac{2\pi}{\nu} = \frac{2\pi}{\sqrt{s_1}}\ell,$$

where T is the period of the resonant Lyapunov orbit. Furthermore, the number ℓ is related to the number of times that the orbit of the choreography winds around a central point. Rational numbers p/q, where q is relatively prime to n, appear infinitely often in an interval, with p and q arbitrarily large. In such a frequency interval, the infinite number of rationals p/q that correspond to choreographies gives arbitrarily large ℓ and m as well. This gives rise to an infinite number of choreographies, with arbitrarily large periods $\frac{2\pi}{\sqrt{s_1}}\ell$, and orbits of correspondingly increasing complexity.

Although the previous results give sufficient conditions for the existence of infinitely many choreographies, there can be additional choreographies due to the fact that the orbit of the choreography $q_n(t)$ has additional symmetries by rotations of $2\pi/m$. We now describe these symmetries and the necessary conditions.

Definition 1 We define a Lyapunov orbit as being $\ell : m$ resonant if it has period

$$T_{\ell:m} = \frac{2\pi}{\sqrt{s_1}}\frac{\ell}{m},$$

where ℓ and m are relatively prime such that

$$k\ell - m \in n\mathbb{Z}.$$

Theorem 1 *In the inertial frame, an $\ell : m$ resonant Lyapunov orbit is a choreography,*

$$(q_j, z_j)(t) = (q_n, z_n)(t + jk'\zeta),$$

where $k' = k - (k\ell - m)\ell'$ with ℓ' the m-modular inverse of ℓ. The projection on the xy-plane of the choreography is symmetric with respect to rotations by an angle $2\pi/m$ and winds around a center ℓ times. The period of the choreography is $m\,T_{\ell:m}$.

Proof Since $u_n(t)$ is 2π-periodic and

$$e^{it\sqrt{s_1}/\nu} = e^{it\ell/m}$$

is $2\pi m$-periodic, the function $q_n(t) = e^{it\sqrt{s_1}/\nu}u_n(t)$ is $2\pi m$-periodic. Furthermore, since

$$q_n(t - 2\pi) = e^{-i2\pi\ell/m}q_n(t), \tag{14}$$

the orbit of $q_n(t)$ is invariant under rotations of $2\pi/m$. By Lemma 1, since

$$\Omega = \frac{k\ell - m}{nm} = \frac{r}{m},$$

with $r = (k\ell - m)/n \in \mathbb{Z}$, the solutions satisfy

$$q_j(t) = e^{-i2\pi j(r/m)} q_n(t + jk\zeta). \tag{15}$$

Since ℓ and m are relatively prime we can find ℓ', the m-modular inverse of ℓ. Since $\ell\ell' = 1 \mod m$, it follows from symmetry (14) that

$$q_n(t - 2\pi jr\ell') = e^{-i2\pi j(r/m)} q_n(t).$$

Therefore,

$$q_j(t) = e^{-i2\pi j(r/m)} q_n(t + jk\zeta) = q_n(t + j(k - rn\ell')\zeta). \tag{16}$$

For the planar component $q_j(t)$ of spatial Lyapunov families, we have the same relation. In addition, we have that the spatial component z_n is 2π-periodic and satisfies $z_j(t) = z_n(t + jk\zeta)$. Since $rn\ell'\zeta = 2\pi r\ell' \in 2\pi\mathbb{Z}$, it follows that

$$z_j(t) = z_n(t + jk\zeta) = z_n(t + j(k - rn\ell')\zeta),$$

and thus, $z_n(t)$ is also $2\pi m$-periodic. □

3 Numerical continuation of Lyapunov families

To continue the Lyapunov families numerically, it is necessary to take the symmetries into account. Equations (1) in the rotational frame have two symmetries that are inherited from Newton's equations in the inertial frame, namely rotations in the plane $e^{\theta i} u_j$ and translations in the spatial coordinate $z_j + c$. This implies that any rotation in the plane and any translation of an equilibrium is also an equilibrium and that the linear equations have two conserved quantities and two trivial eigenvalues.

To determine the conserved quantities, we can sum equation (1) over the z_j coordinates to obtain that $\sum_{j=1}^{n} \ddot{z}_j = 0$, i.e., the linear momentum in z is conserved,

$$\sum_{j=1}^{n} \dot{z}_j(t) = \text{constant}. \tag{17}$$

The other conserved quantity can be obtained easily in real coordinates. Identifying i with the symplectic matrix J, taking the real product of the u component of Eq. (1) with the generator of the rotations Ju_j, and summing over j, we obtain

$$0 = \sum_{j=1}^{n} \left\langle \ddot{u}_j + 2\sqrt{s_1} J\dot{u}_j, Ju_j \right\rangle_{\mathbb{R}^2} = \frac{d}{dt} \sum_{j=1}^{n} \left\langle \dot{u}_j + \sqrt{s_1} Ju_j, Ju_j \right\rangle_{\mathbb{R}^2}.$$

Therefore, the second conserved quantity is

$$\sum_{j=1}^{n} \dot{u}_j \cdot Ju_j - \sqrt{s_1} \left| u_j \right|^2.$$

To continue the Lyapunov families numerically, we need to take the conserved quantities into account. Let $x_j = (u_j, z_j)$ be the vector of positions and $v_j = (\dot{u}_j, \dot{z}_j)$ the vector of velocities. In our numerical computations, we use the augmented equations

$$\dot{x}_j = v_j,$$

$$\dot{v}_j = 2\sqrt{s_1}\,\mathrm{diag}(J,0)\,v_j + \nabla_{x_j} V + \sum_{k=1}^{3} \lambda_k F_j^k, \tag{18}$$

where $F_j^1 = e_3$ corresponds to the generator of the translations in z, $F_j^2 = diag(J,0)x_j$ to rotations in the plane, and $F_j^3 = v_j$ to the conservation of the energy. The solutions of Eq. (18) are solutions of the original equations of motion when the values of the three parameters λ_k are zero. It is known that the converse of this statement is also true (for instance see Ize and Vignoli (2003) and Muñoz-Almaraz et al. (2003)).

Proposition 3 *Assume that the functions $F^k = (F_1^k, \ldots, F_n^k)$ for $k = 1, 2, 3$, are orthogonal (or linearly independent). Then, a solution (x, v) of the equation is a solution of augmented Eq. (18) if and only if $\lambda_j = 0$ for $j = 1, 2, 3$.*

Proof By scalar multiplication of the equation in (18) by F_j^k, summing over j, and integrating by parts, we obtain

$$\int_0^{2\pi} \sum_{j=1}^{n} \dot{v}_j \cdot F_j^k \mathrm{d}t = \lambda_k \int_0^{2\pi} \sum_{j=1}^{n} \left| F_j^k \right|^2 \mathrm{d}t.$$

Suppose that (x, v) is a solution. Then, it conserves the aforementioned quantities, and therefore

$$\int_0^{2\pi} \sum_{j=1}^{n} \dot{v}_j \cdot F_j^k \mathrm{d}t = 0.$$

The result that $\lambda_j = 0$ then follows from the orthogonality of the fields F^k. □

For the purpose of numerical continuation, the period of the solutions is rescaled to 1, so that it appears explicitly in the equations. Let $\varphi(t, x, v)$ be the flow of the rescaled equations. Then, we define the time-1 map for the rescaled flow as

$$\varphi(1, x, v; T, \lambda_1, \lambda_2, \lambda_3) : \mathbb{R}^{6n} \times \mathbb{R}^4 \to \mathbb{R}^{6n}.$$

Let $X(t)$ be the solution computed in the previous step along a family. We implement Poincaré restrictions given by the integrals

$$I_1 = \int_0^1 x_n \cdot e_2 \,\mathrm{d}t = 0, \quad I_2 = \int_0^1 x_n \cdot e_3 \,\mathrm{d}t = 0,$$
$$I_3 = \int_0^1 (x_n(t) - X_n(t)) \cdot \dot{X}_n(t) \,\mathrm{d}t = 0,$$

which correspond to rotations, translations in z, and the energy, respectively.

The results in Muñoz-Almaraz et al. (2003) are based on the continuation of zeros of the map

$$F(x, v; T, \lambda_1, \lambda_2, \lambda_3) := ((x, v) - \varphi(x, v), I_1, I_2, I_3) : \mathbb{R}^{6n+4} \to \mathbb{R}^{6n+3}.$$

Actually, continuation is done with AUTO for the complete operator equation in function space. That is, the numerical computation of the maps φ and I_j is done for the corresponding operators in $C^2_{2\pi}(\mathbb{R}^{6n})$. This operator equation is discretized using highly accurate piecewise polynomial collocation at Gauss points.

4 Lyapunov families and bifurcating families

In this section, we give a brief description of some of the many solution families that we have computed using python scripts that drive the AUTO software. We start with Planar families that arise from the circular, polygonal equilibrium state of the n-body problem when $n \geq 6$. For the case $n = 6$, there is a single such Planar family. While of interest, its orbits are of relatively small amplitude, and for this reason, we have chosen to illustrate the numerical results for the case $n = 7$ in this section. One of the four Planar families that exist for $n = 7$ also consists of relatively small amplitude orbits. The other three Planar families are illustrated in Fig. 1, where the panels on the left show an orbit along each of three distinct Planar Lyapunov families. These orbits are well away from the polygonal relative equilibrium from which the respective families originate, while they are also still well away from the collision orbits which these families appear to approach. The panels on the right in Fig. 1 show orbits along the three families that are further away from the relative equilibria. Orbits along the Planar families for the cases $n = 8$ and $n = 9$ share many features with those for the case $n = 7$.

Families of spatial orbits, which have nonzero z-component, emanate from the polygonal relative equilibrium when $n \geq 3$. These families and their orbits are often referred to as " Vertical," because the solution of the linearized Newton equations at the equilibrium is perfectly Vertical, i.e., the x- and y-components are identically zero. For the case $n = 3$, the Vertical Lyapunov family is highly degenerate, as it corresponds to an eigenvalue of algebraic multiplicity 5, and there are no further eigenvalues that give rise to Vertical orbits. For the case $n = 4$, there is an equally degenerate eigenvalue ($k = 1$). However, there is also a nondegenerate eigenvalue that gives rise to a Vertical family, namely the one known as the "Hip-Hop family" ($k = 2$). The top-left panel of Fig. 2 shows orbits along this family, which terminates in a collision orbit. The coloring of the orbits along the family gradually changes from solid blue (near the equilibrium) to solid red (near the terminating collision orbit). The same coloring scheme is used when showing other entire families of orbits in rotating coordinates. The top-right panel of Fig. 2 shows a single orbit from the Hip-Hop family, namely the first bifurcation orbit encountered along it. The color of this orbit gradually changes from blue to red as the orbit is traversed, so that one can infer the direction of motion. The masses are shown at their "initial" positions. The same coloring scheme is used when showing other individual orbits in rotating coordinates.

The center-left panel of Fig. 2 shows the Axial family that bifurcates from the Hip-Hop family. The name "Axial" alludes to the fact that the orbits of this family are invariant under the transformation $(-y, -z)$, when the x-axis is chosen to pass through the "center" of the orbit. The Axial family connects to a Planar family, namely at the Planar bifurcation orbit shown in the center-right panel of Fig. 2. We refer to this Planar family as "Unchained," because some of its orbits give rise to choreographies called "Unchained polygons" in Chenciner and Féjoz (2009). The Hip-Hop family for $n = 4$, and its bifurcating families, are qualitatively similar to corresponding families that we have computed for the cases $n = 6$ and $n = 8$.

The examples of orbit families given in this section are representative of the many Planar and spatial Lyapunov families that we have computed, their secondary and tertiary bifurcating families, as well as corresponding families for other values of n. Complete bifurcation pictures are rather complex, but our algorithms are capable of attaining a high degree of detail, which at this point excludes only the degenerate bifurcations mentioned earlier.

In the following sections, we focus our attention on choreographies that arise from resonant periodic orbits. The statements proved for the Lyapunov families also hold true for subsequent

spatial and planar bifurcations, as long as symmetries (3) and (5) are present. Figure 3 illustrates the appearance of choreographies from resonant Lyapunov orbits and from resonant orbits along subsequent bifurcating families. Specifically, the top-left panel of Fig. 3 shows a resonant Planar Lyapunov orbit for the case $n = 7$, and the top-right panel shows the same orbit in the inertial frame, where it is seen to correspond to a choreography. Similarly, the center panels show a resonant spatial Lyapunov orbit and corresponding choreography for $n = 9$, while the bottom panels show a resonant Axial orbit and corresponding choreography for $n = 4$.

5 Choreographies along Planar Lyapunov families

In this section, we present some of the infinitely many choreographies that appear along the Planar Lyapunov families, namely for the cases $n = 7$, $n = 8$ and $n = 9$, as shown in Figs. 4 and 5, respectively. Corresponding data are given in Tables 1, 2 and 3. Each choreography winds ℓ times around a center and is invariant under rotations of $2\pi/m$. The bodies move in groups of d-polygons, where d is the greatest common divisor of n and k. In addition, these choreographies are symmetric with respect to reflection in the plane generated by the second symmetry in (3).

When there is an infinite number of choreographies, then the winding number ℓ and the symmetry indicator m can be arbitrarily large and the choreography arbitrarily complex. From the observed range of values of the periods along a Lyapunov family, we mostly choose the simpler resonances and hence the simpler choreographies. For example, the family $k = 2$ for $n = 7$ has a relatively simple choreography. Here, $\ell = 5$ and $m = 3$ are relatively prime, with

$$k\ell - m = 2 \times 5 - 3 = 7 \in n\mathbb{Z}.$$

In this example, $2\pi s_1^{-1/2} = 4.1387$, and since $T_{5:3} = (2\pi s_1^{-1/2})(5/3) = 6.8978$ is within the range of periods of the Lyapunov family, it follows that the 5:3 resonant Lyapunov orbit corresponds to a choreography in the inertial frame. Similar statements apply to other planar choreographies.

The choreography for $n = 7$, with $k = 2$ and resonance 5:3, is shown in the top-left panel of Fig. 4. It has period $3T_{5:3}$, winding number 5, and it is invariant under rotations by $2\pi/3$. For $n = 7$, there is in fact a sequence of Planar Lyapunov families, having $k = 2, 3, 4, 2$, respectively. Two more choreographies for $n = 7$, with $k = 3$ and $k = 4$, are shown in the top-right and center-left panels of Fig. 4. For $n = 8$, there is a sequence of Planar Lyapunov families having $k = 2, 3, 4, 5, 2$, respectively. We have chosen four choreographies from these families for different k, as included in Figs. 4 and 5. Similarly, for $n = 9$ there is a sequence of Planar Lyapunov families having $k = 2, 3, 4, 5, 6, 2$, respectively. Figure 5 includes five choreographies for different k from these families.

6 Choreographies along Vertical Lyapunov families and their bifurcating families

In this section, we give examples of choreographies along the Vertical Lyapunov families and along their bifurcating families. The projections of these choreographies onto the xy-plane are invariant under rotations of $2\pi/m$. The bodies form groups of d-polygons, where d is the

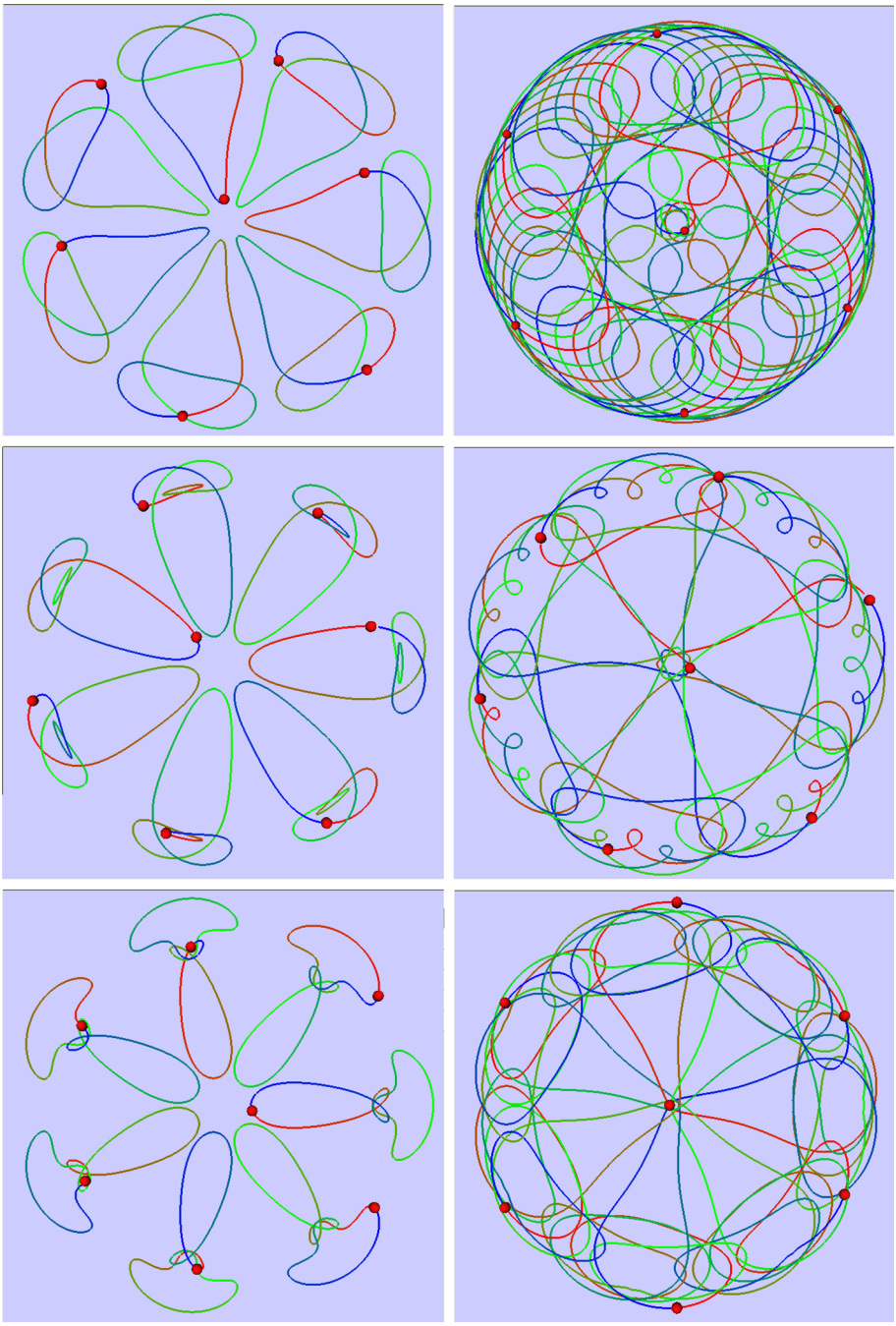

Fig. 1 Some orbits along Planar families for the case $n = 7$. The color ranges from blue to red according to the time for one period to be completed. Top: two orbits with $k = 2$. Center: two orbits with $k = 3$. Bottom: two orbits with $k = 4$

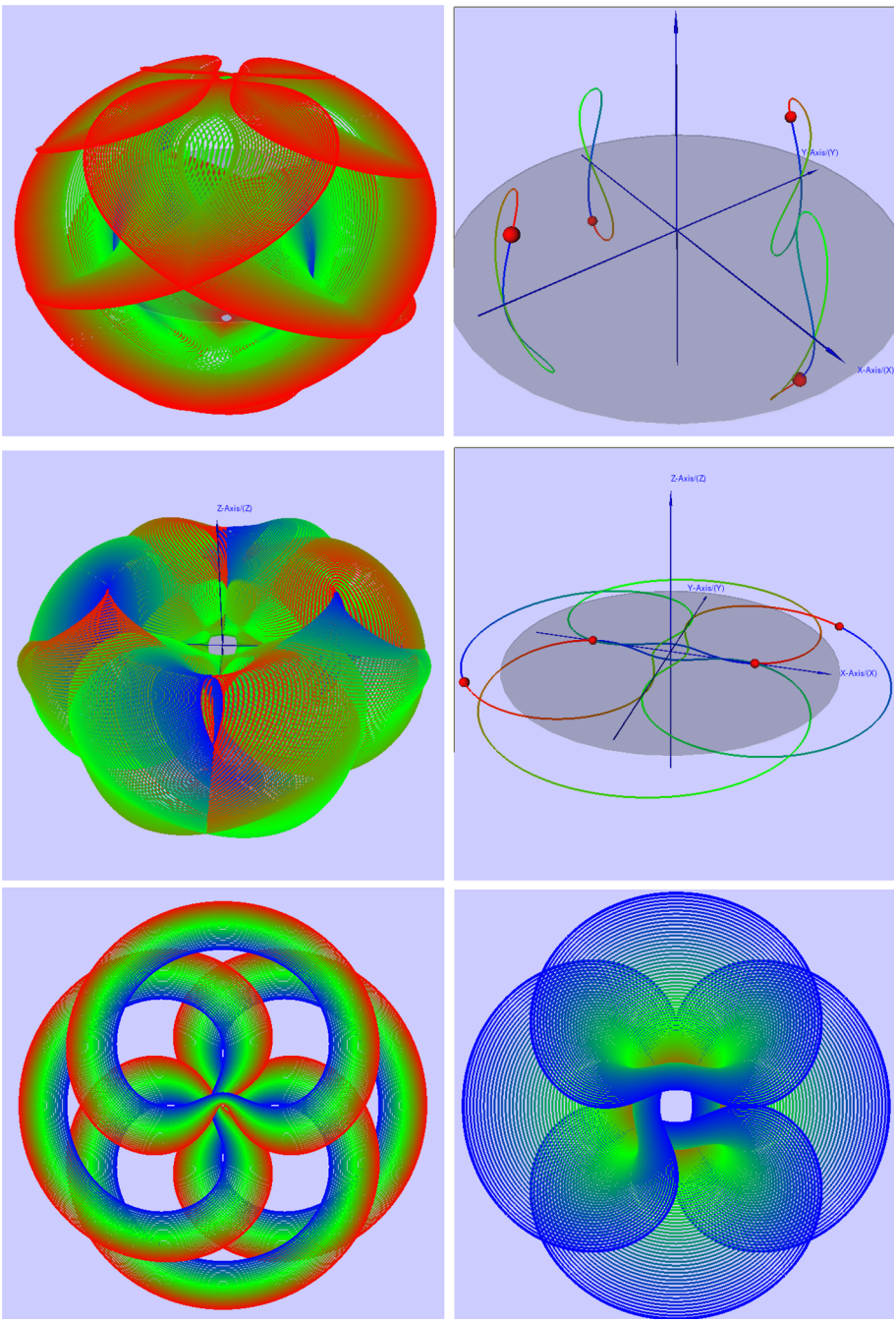

Fig. 2 Top left: the vertical Lyapunov family for $n = 4$ and $k = 2$. Top right: the first bifurcation orbit along the Vertical family. Center left: the Axial family that bifurcates from the Vertical family. Center right: the bifurcation orbit where the Axial family connects to a Planar family. Bottom left: one branch of the Planar family to which the Axial family connects. Bottom right: the other branch of the family to which the Axial family connects

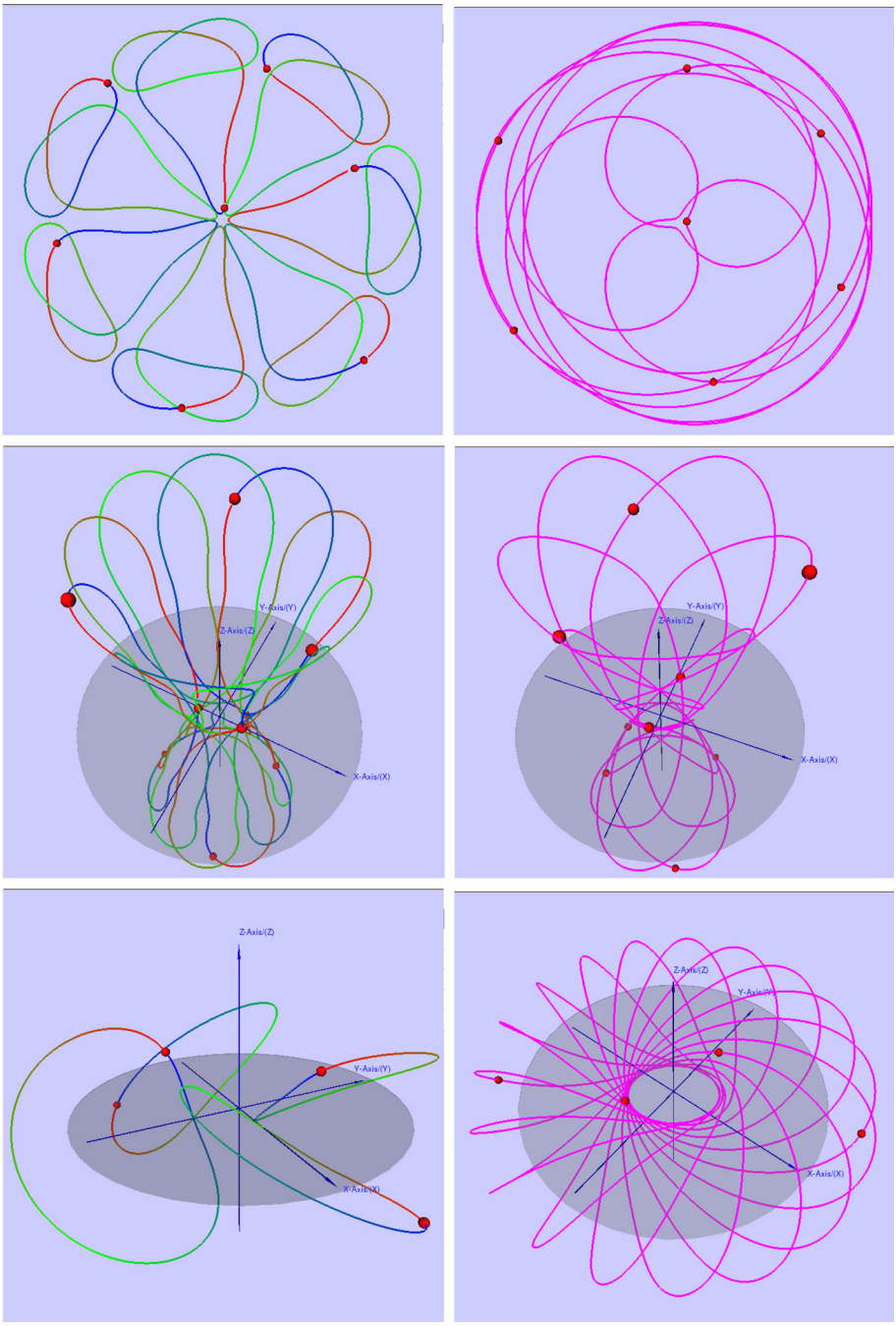

Fig. 3 The panels on the left show orbits in the rotating frame, while the panels on the right show the same orbits in the inertial frame, where they correspond to choreographies. Top: a resonant Planar Lyapunov orbit. Center: a resonant Vertical Lyapunov orbit. Bottom: a resonant Axial orbit

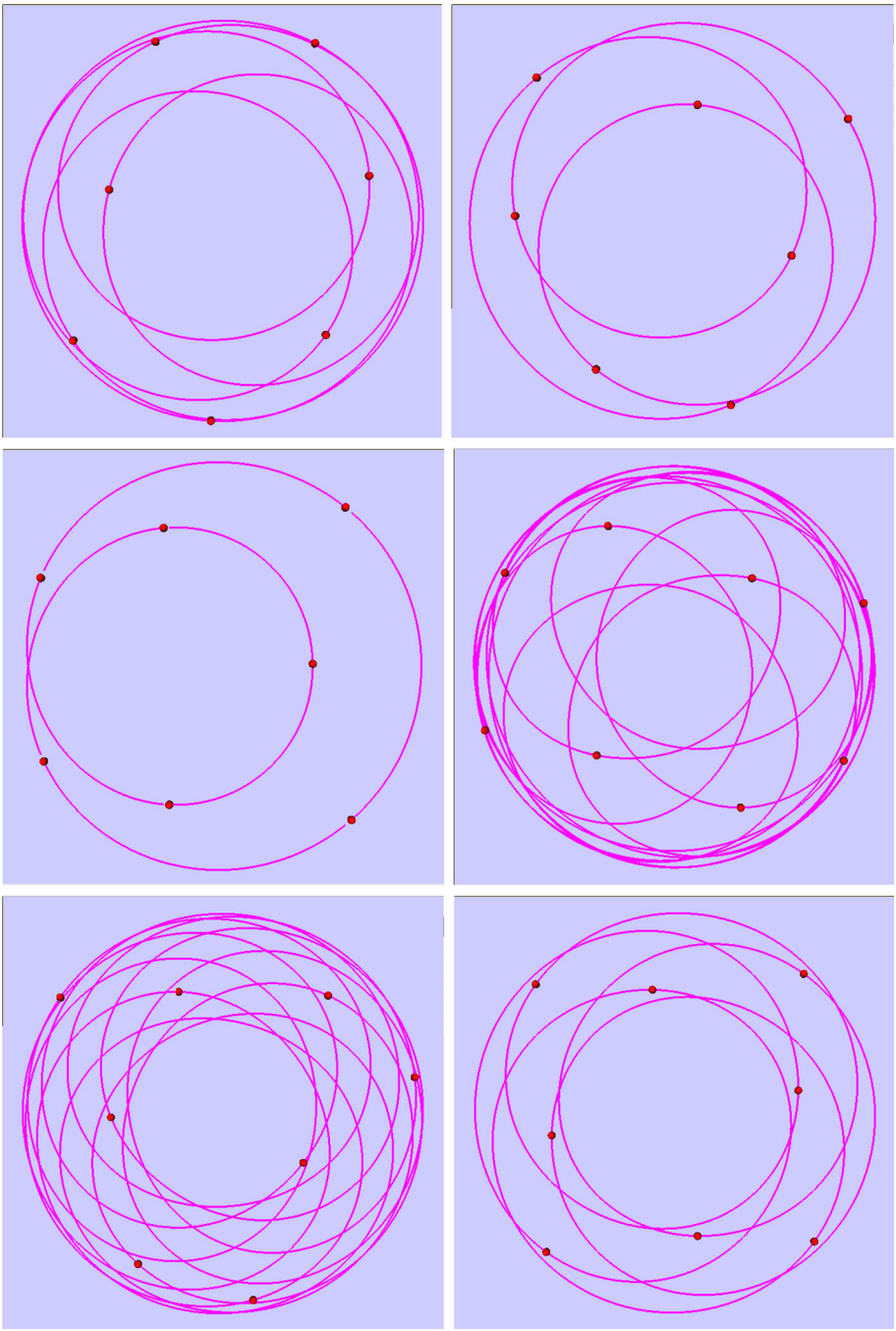

Fig. 4 Top left: a 5:3-resonant orbit for $k = 2$ and $n = 7$. Top right: a 3:2-resonant orbit for $k = 3$ and $n = 7$. Center left: a 2:1-resonant orbit for $k = 4$ and $n = 7$. Center right: a 11:6-resonant orbit for $k = 2$ and $n = 8$. Bottom left: a 11:9-resonant orbit for $k = 3$ and $n = 8$. Bottom right: a 5:4-resonant orbit for $k = 4$ and $n = 8$

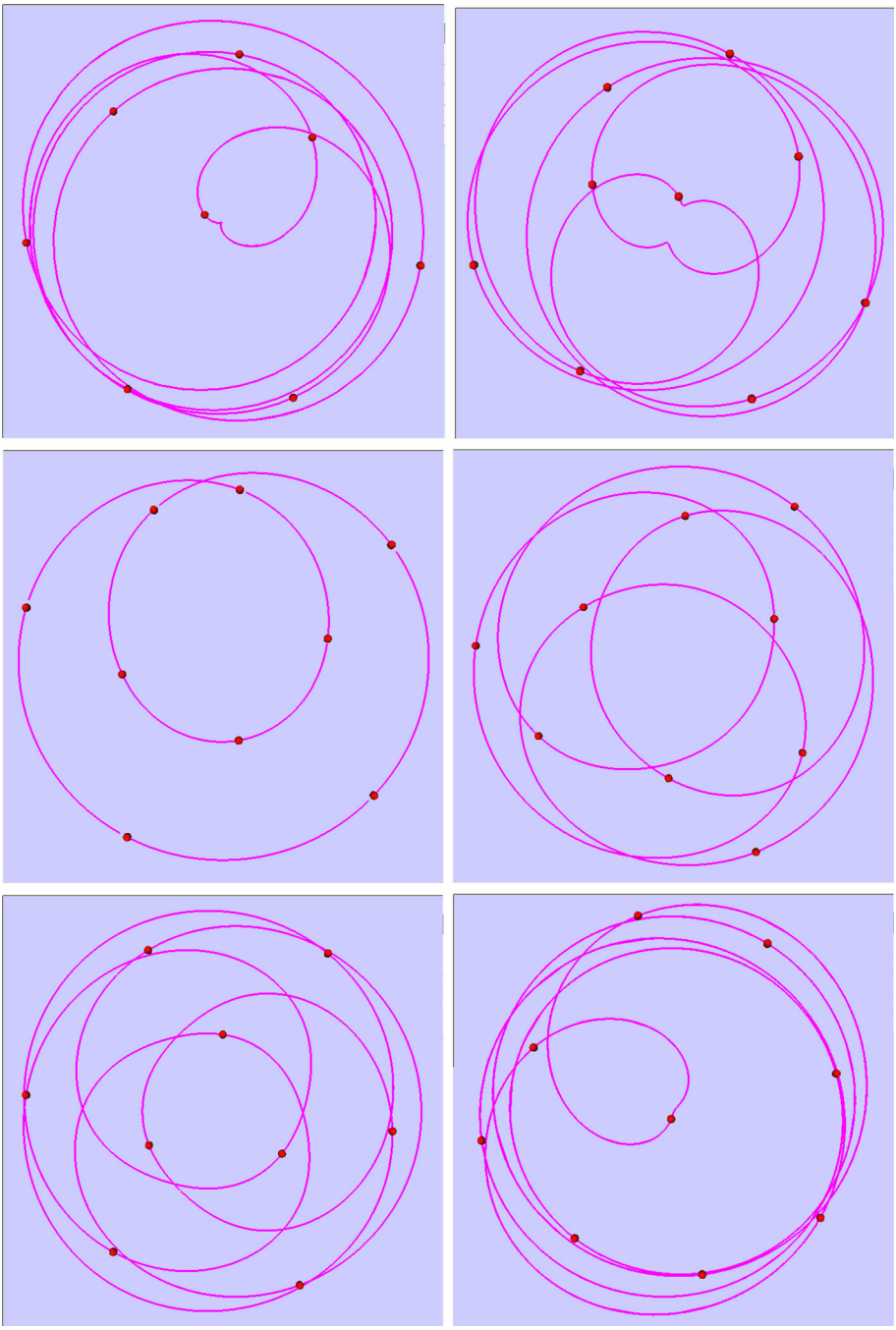

Fig. 5 Top left: a 5:1-resonant orbit for $k = 5$ and $n = 8$. Top right: a 5:2-resonant orbit for $k = 4$ and $n = 9$. Center left: a 2:1-resonant orbit for $k = 5$ and $n = 9$. Center right: a 4:3-resonant orbit for $k = 3$ and $n = 9$. Bottom left: a 5:3-resonant orbit for $k = 6$ and $n = 9$. Bottom right: a 5:1-resonant orbit for $k = 2$ and $n = 9$

Table 1 Data for $n = 7$ bodies

k	Eigenvalue	Period interval	Resonant orbit
2	$1.53960i$	[4.0811, 28.328]	5:3
3	$1.85058i$	[3.3953, 27.974]	3:2
4	$1.50806i$	[4.1664, 28.499]	2:1
2	$0.761477i$	[8.2513 ,8.3328]	–

Table 2 Data for $n = 8$ bodies

k	Eigenvalue	Period interval	Resonant orbit
2	$1.94947i$	[3.2230, 14.836]	11:6
3	$2.39714i$	[2.6211, 29.654]	11:9
4	$2.41171i$	[2.6053, 7.4935]	5:4
5	$1.91468i$	[3.2814, 29.122]	5:1
2	$0.435437i$	[5.4804, 14.430]	–

greatest common divisor of n and k. Since we obtain choreographies by rotating closed orbits, each choreography is contained in a surface of revolution. Indeed, due to the symmetries of the Vertical families, the choreographies wind around a cylindrical manifold with winding number ℓ, while for the Axial families the choreographies wind around a toroidal manifold with winding numbers ℓ and m.

The spatial choreographies along the Vertical Lyapunov families are symmetric with respect to the reflections $-y$ and $-z$, when the x-axis is chosen to pass through the "center" of the orbit. While planar choreographies for large values of ℓ and m are somewhat difficult to appreciate, spatial choreographies of this type are easier to visualize because they wind around a cylindrical manifold. For even values of n, we mention the case $k = n/2$, for which the orbits of the Vertical family are known as Hip-Hop orbits. Choreographies along such families have been described before in Terracini and Venturelli (2007) and in Chenciner and Féjoz (2009), where they were found numerically as local minimizers of the action restricted to symmetric paths. Along Hip-Hop families, we have located the choreography for $n = 4$ found in Terracini and Venturelli (2007). Several choreographies along Hip-Hop families are shown the top four panels of Fig. 6. We have not computed all Vertical families that are not Hip-Hop families, due to the presence of double resonant eigenvalues. We show choreographies along some of these resonant Vertical families, namely in the bottom panels of Fig. 6 for $n = 9$ and in the center panels of Fig. 8 for $n = 7$. Such families were not determined in Chenciner and Féjoz (2009) because they do not correspond to local minimizers of the action. Further investigation is needed for a systematic approach to determine these families.

We have also determined choreographies along families that emanate from the first bifurcation along Vertical families in the rotating frame, namely the Axial families. The projections of these spatial choreographies onto the xy-plane are somewhat similar to those along the Planar Lyapunov orbits. However, the spatial periodic orbits in the rotating frame that correspond to these choreographies have only one symmetry, which is given by the transformation $(-y, -z)$, when the x-axis is chosen to pass through the "center" of the orbit in the rotating frame; see the bottom-left panel of Fig. 3. This is due to the fact that the Axial family arises from the Vertical Lyapunov family via a symmetry-breaking bifurcation. The symmetry implies that choreographies along the Axial families wind around a toroidal manifold with

Table 3 Data for $n = 9$ bodies

k	Eigenvalue	Period interval	Resonant orbit
2	$2.27175i$	[2.7660, 30]	5:1
3	$2.85442i$	[2.2012, 10.298]	4:3
4	$3.06012i$	[2.0534, 30.411]	5:2
5	$2.90713i$	[2.1613, 30.612]	2:1
6	$2.26399i$	[2.7197, 10.008]	5:3
2	$0.196565i$	[15.400, 31.927]	–

winding numbers ℓ and m. Since we assume that ℓ and m are co-prime, the choreography path is known as a *torus knot*. The simplest nontrivial example is the (2, 3)-torus knot, also known as the *trefoil knot*. We note that for other integers ℓ and m such that $k\ell - m \notin n\mathbb{Z}$, the orbit of the n bodies in the inertial frame consists of separate curves that form a torus link.

Some of the choreographies along the Axial families are shown in Fig. 7 for $n = 4, 6, 8$. For the cases $n = 7, 9$, we have found bifurcating families with axial symmetries similar to $n = 4, 6, 8$. The case of seven bodies is particularly interesting, since along the Axial family with $k = 2$ we find a Figure-Eight choreography that corresponds to a $1 : 2$ resonant Lyapunov orbit; see the bottom panels of Fig. 8. The tori that contain the Axial family in the inertial frame become degenerate at the $1 : 2$ resonant orbit. By degenerate, we mean that the inner circle of the torus in the plane xy collapses into the origin. Moreover, the $1 : 2$ choreography is a torus knot that corresponds to a Figure-Eight in the plane xz, which is classified as $D'(7, 2)$ in Montaldi and Steckles (2013).

In Sect. 4, we already mentioned that there are Planar bifurcation orbits along Axial families that give rise to Planar families. Such an Axial family and its planar bifurcation orbit are shown in the center panels of Fig. 2, namely for the case $n = 4$. Orbits along the two branches of the bifurcating Planar family are shown in the bottom panels. Specifically, our numerical computations indicate that Hip-Hop families connect indirectly to Planar families via the above-described tertiary bifurcation. Choreographies along such Planar families have symmetries that are similar to those of Planar Lyapunov families, although in fact these families do not correspond to Lyapunov families. While there are no Planar Lyapunov families for $n = 4, 5$, and 6, there are such tertiary Planar families for these values of n, and these contain planar choreographies. Such choreographies are called unchained polygons in Chenciner and Féjoz (2009), and there are infinitely many of these. In particular, the Vertical family for $n = 3$ and $k = 1$ leads indirectly to the Planar P_{12}-family of Marchal (2000). We have continued such families numerically for $k = n/2$, where $n = 4, 6$, and 8, and six choreographies along them are shown in the panels of Fig. 9.

7 Numerical continuation from other configurations

7.1 The Maxwell configuration

The choreographies in the preceding sections are unstable, in part because they arise directly or indirectly from an unstable relative equilibrium. To determine more stable solutions, it is helpful to consider orbits that emanate from a stable relative equilibrium. The polygonal equilibrium is never stable; about half of its eigenvalues are stable and about half are unstable. For this reason, we also considered the Maxwell configuration, consisting of an n-polygon

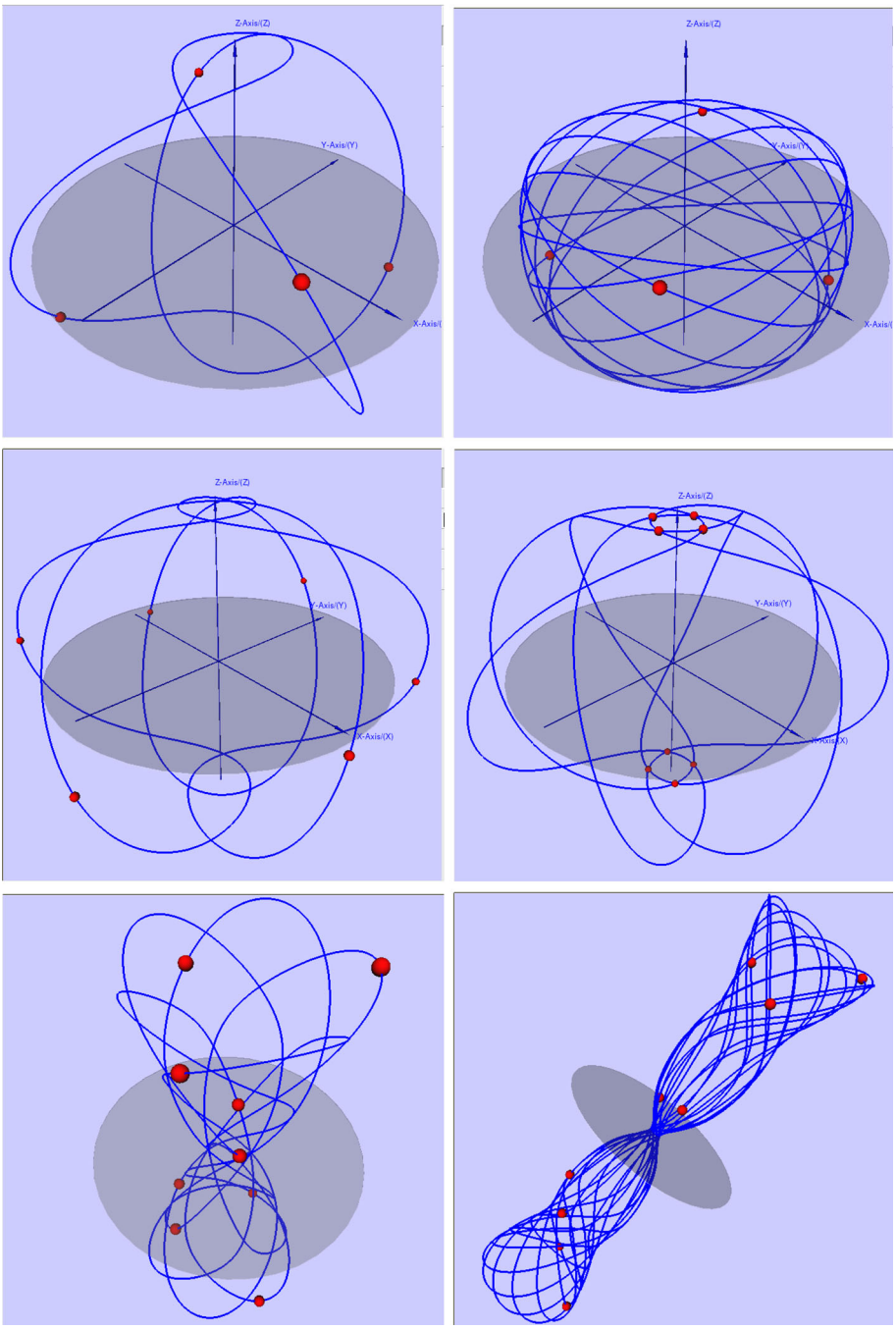

Fig. 6 Vertical Lyapunov families. Top left: a 3:2-resonant Hip-Hop orbit along V_1 for $n = 4$. Top right: a 9:10-resonant Hip-Hop orbit along V_1 for $n = 4$. Center left: a 5:3-resonant Hip-Hop along V_1 for $n = 6$. Center right: a 7:4-resonant Hip-Hop along V_1 for $n = 8$. Bottom left: an 11:5 resonance along V_3 for $n = 9$. Bottom right: a 31:10 resonance along V_3 for $n = 9$

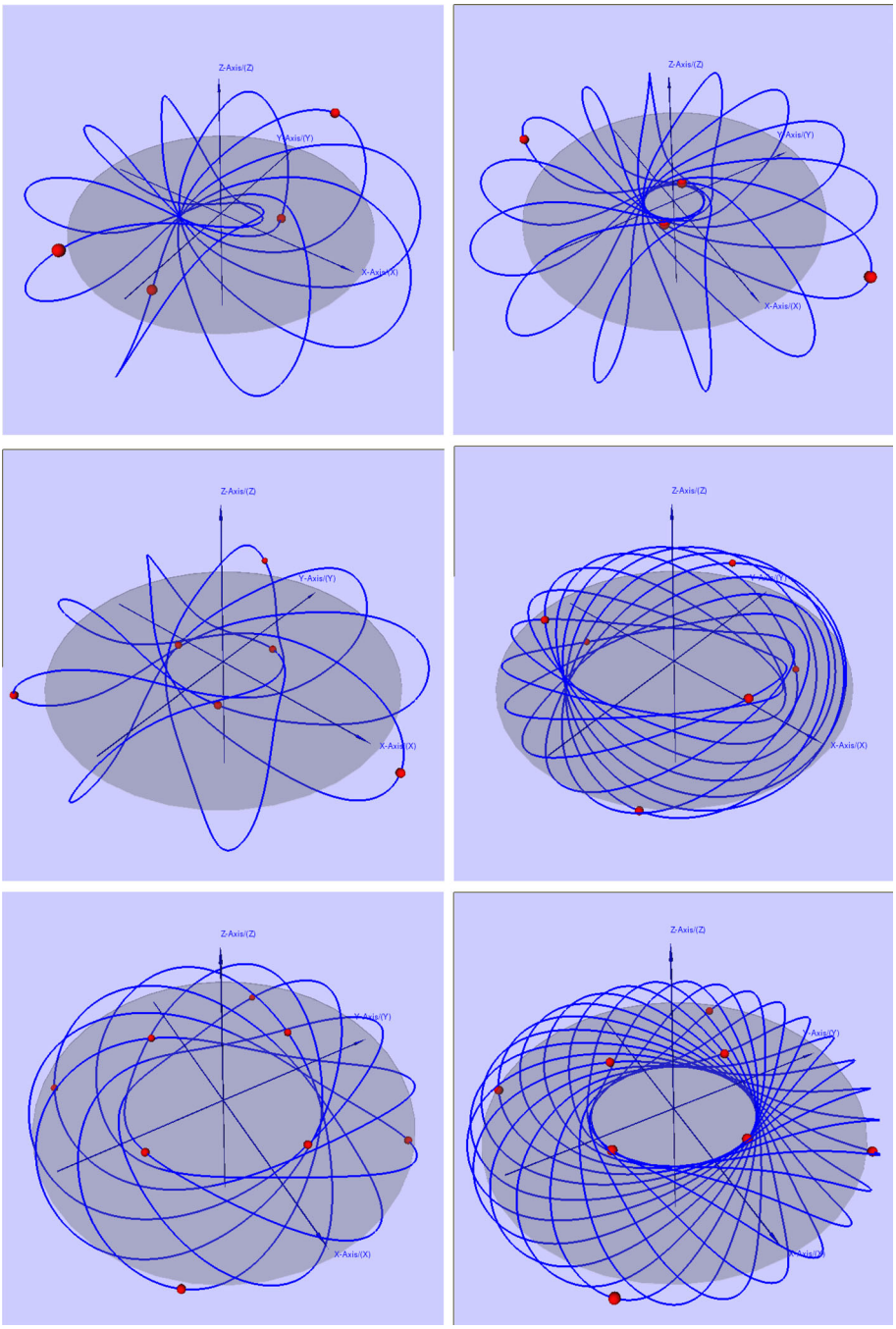

Fig. 7 Resonant Axial orbits with $k = n/2$. Top left: a 7:10 resonant Axial orbit for $n = 4$. Top right: a 9:14 resonant Axial orbit for $n = 4$. Center left: a 5:9 resonant Axial orbit for $n = 6$. Center right: an 11:15 resonant Axial orbit for $n = 6$. Bottom left: a 7:12 resonant orbit for $n = 8$. Bottom right: a 15:28 resonant Axial orbit for $n = 8$

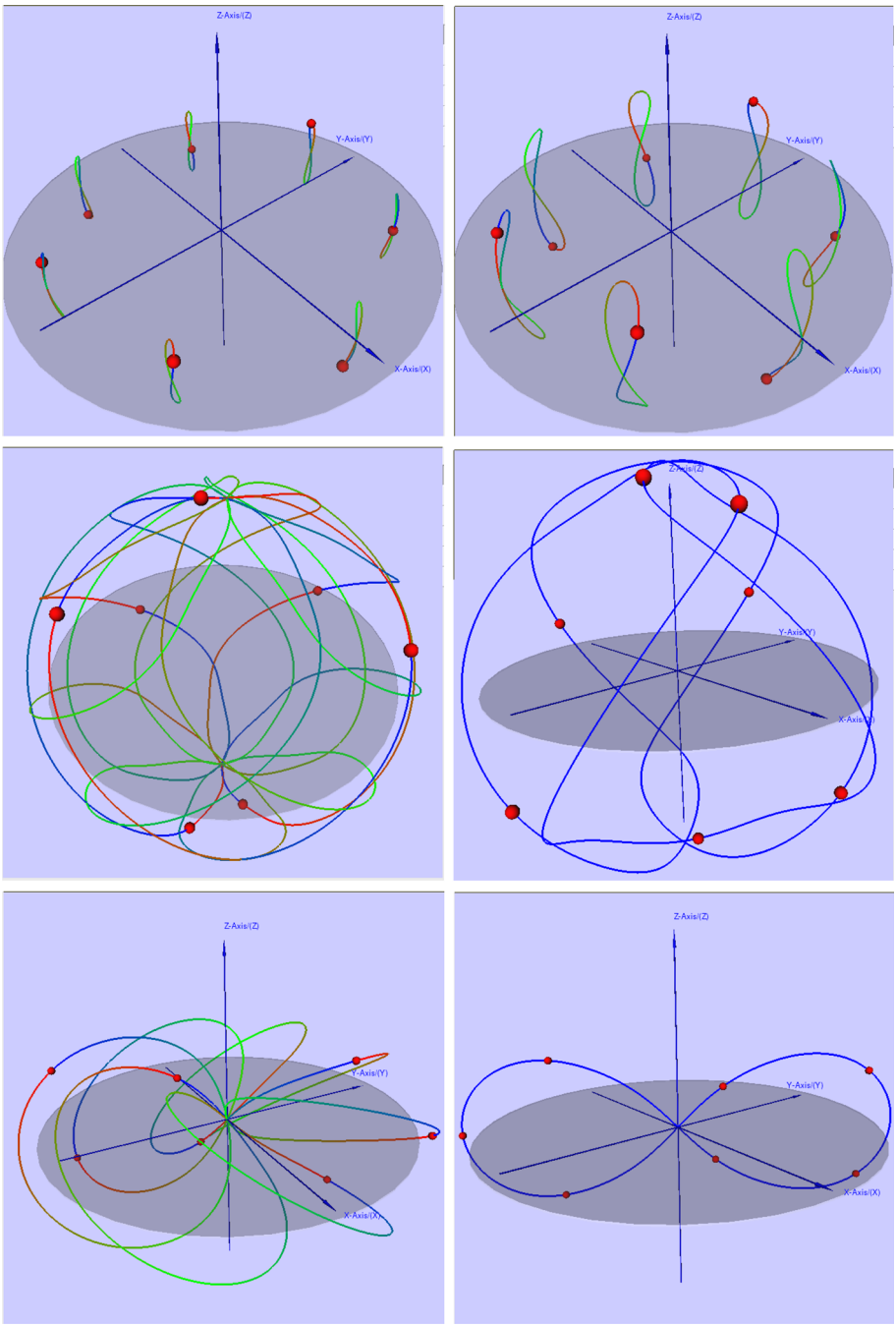

Fig. 8 Connecting families from the heptagon to the Figure-Eight choreography for seven bodies ($n = 7$). Top left: an orbit along the Vertical family with $k = 2$. Top right: the bifurcation orbit that gives rise to an Axial family. Center left: a 5:3-resonant orbit along the Vertical family. Center right: the choreography that corresponds to the 5:3 resonant orbit. Bottom left: the 1:2 resonant orbit along the bifurcating Axial family. Bottom right: the Figure-Eight choreography that corresponds to the 1:2 resonant orbit along the bifurcating Axial family

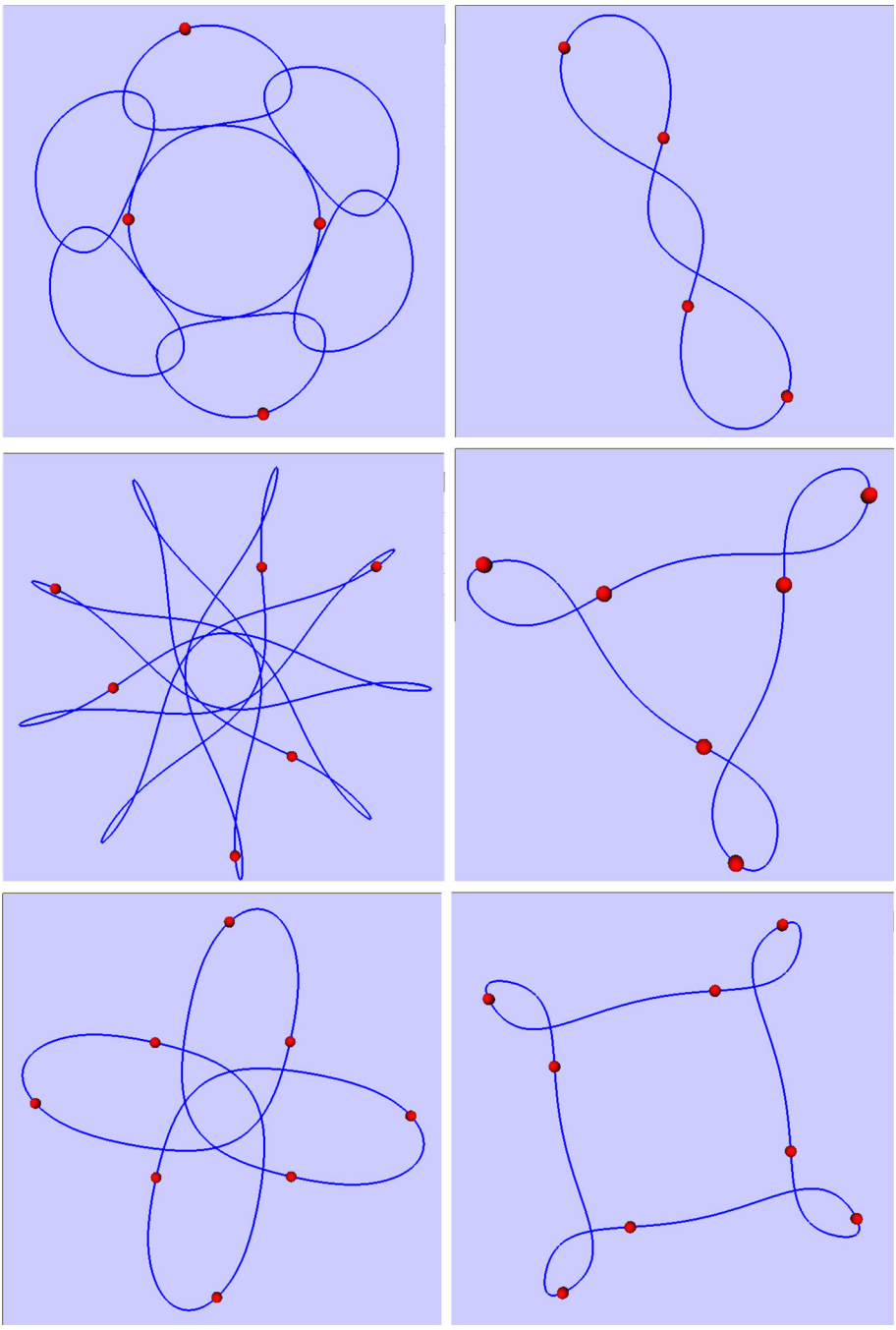

Fig. 9 Unchained polygons for $k = n/2$. Top left: a 1:6 resonant orbit for $n = 4$. Top right: a 1:2 resonant orbit for $n = 4$. Center left: a 5:9 resonant orbit for $n = 6$. Center right: a $1 : 3$ resonant orbit for $n = 6$. Bottom left: a 3:4 resonant orbit for $n = 8$. Bottom right: a 1:4 resonant orbit for $n = 8$

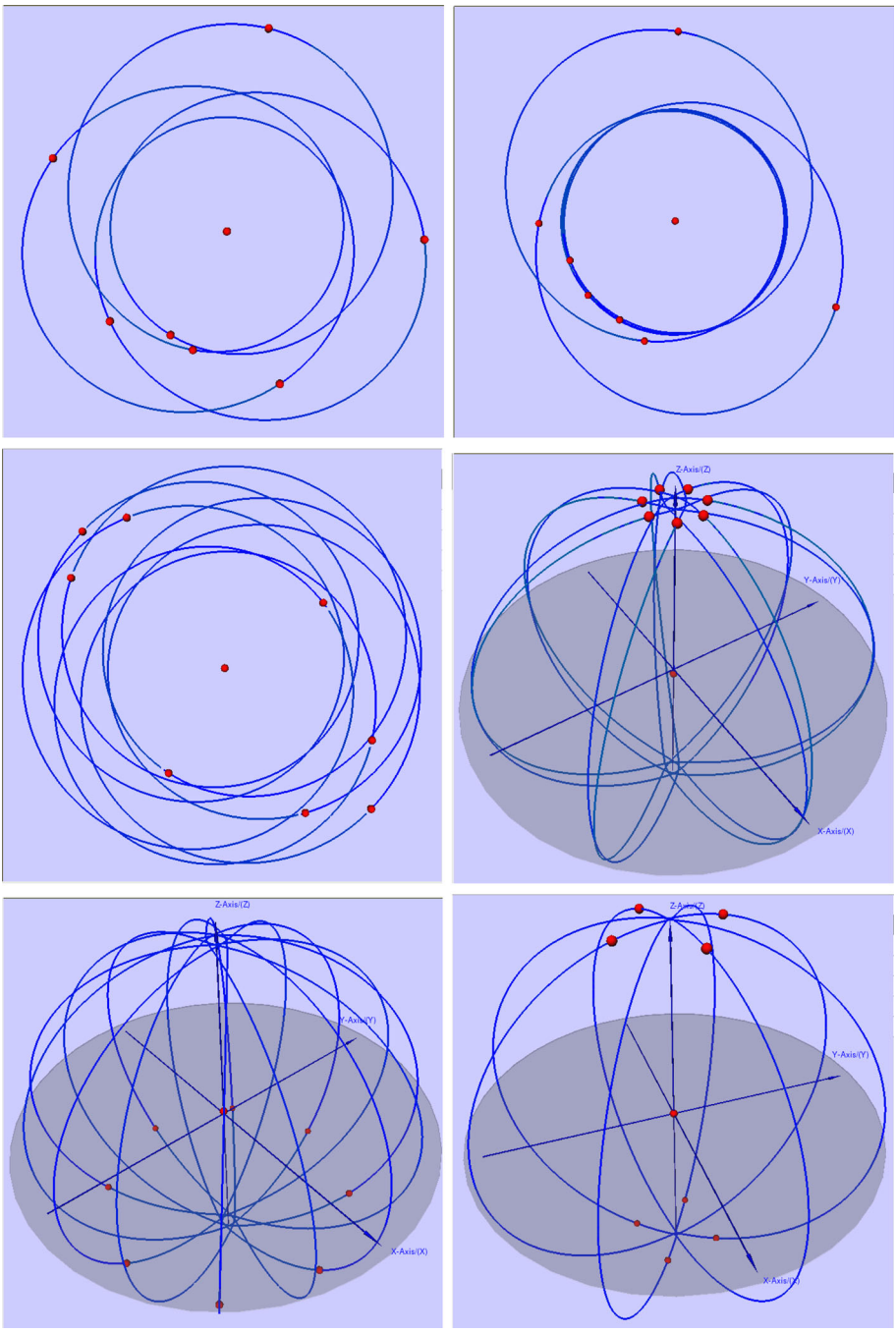

Fig. 10 Top left: a 4:3 resonant orbit for $7+1$ bodies and $k=6$. Top right: a 5:2 resonant orbit for $7+1$ bodies and $k=6$. Center left: a 7:3 resonant orbit for $8+1$ bodies for $k=8$. Center right: an 8:7 resonant orbit for $7+1$ bodies and $k=7$. Bottom left: a 9:8 resonant orbit for $8+1$ bodies and $k=8$. Bottom right: a 15:12 resonant orbit for $8+1$ bodies and $k=4$. Although not quite visible in these panels, the central body also executes a small, nontrivial orbit

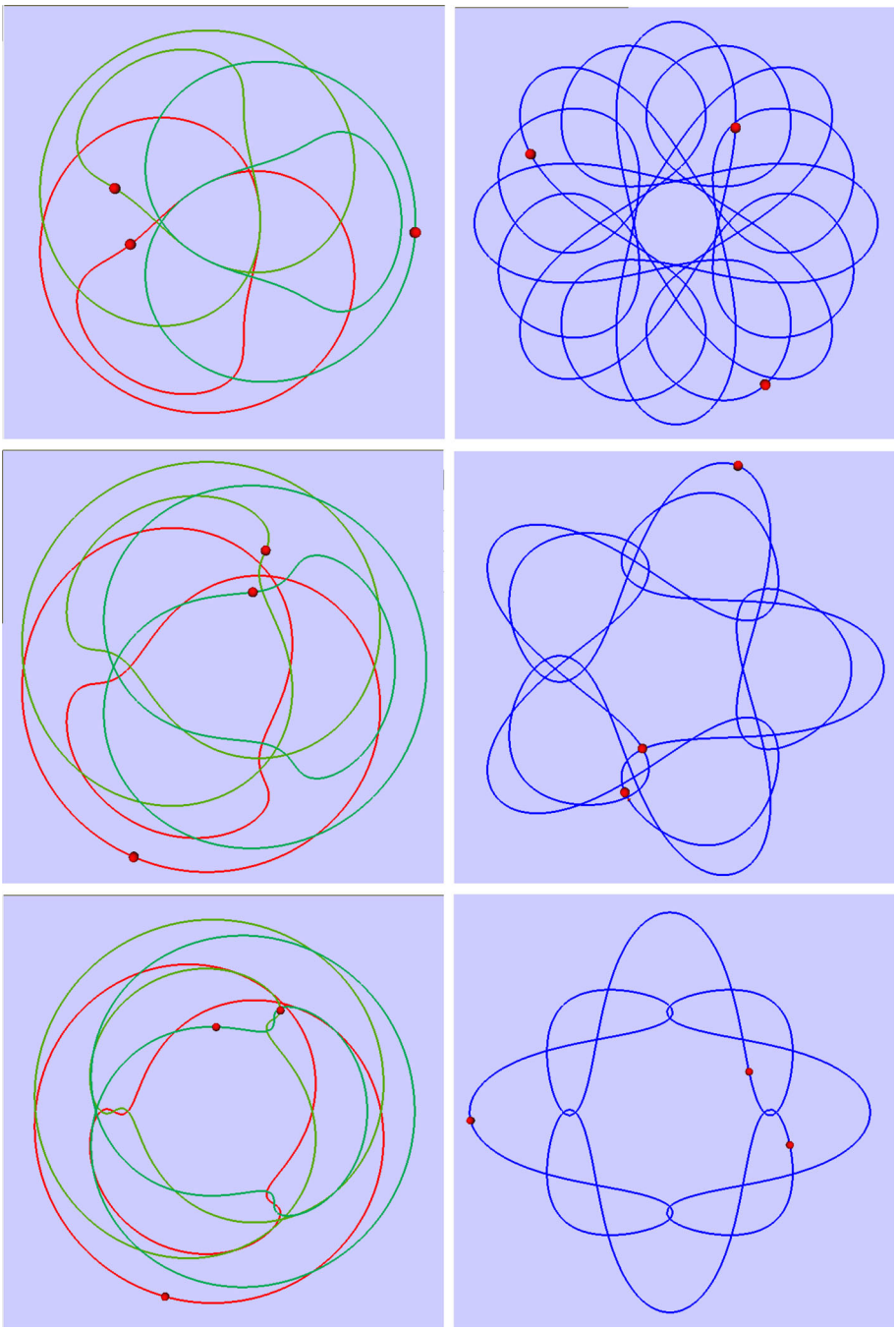

Fig. 11 The panels on the left show orbits which are resonant along the Planar family from the Figure-Eight in the rotating frame, while the panels on the right show the same orbits in the inertial frame, where they correspond to choreographies. Top: An 11:8 resonant orbit along the Planar family. Center: An 8:5 resonant orbit along the Planar family. Bottom: A 7:4 resonant orbit along the Planar family

with an additional massive body at the center. This equilibrium is known to be stable when $n \geq 7$. Specifically, the central body has mass $m_0 = \mu$, and the other n bodies have equal mass $m_j = 1$ for $j \in \{1, \ldots, n\}$. Let $(q_j, z_j) \in \mathbb{C} \times \mathbb{R}$ be the position of body $j \in \{0, 1, \ldots, n\}$. The Newton equations of motion for the $n+1$ bodies in rotating coordinates $q_j(t) = e^{i\sqrt{\omega}t} u_j(t)$ have an equilibrium with $(u_0, z_0) = (0, 0)$ and $\left(u_j, z_j\right) = \left(e^{ij\zeta}, 0\right)$ for $j \in \{1, \ldots, n\}$ when $\omega = \mu + s_1$. This well-known Maxwell configuration reduces to the polygonal relative equilibrium when $\mu = 0$.

For $n \geq 7$, all planar eigenvalues are imaginary and produce Planar Lyapunov families. The $n+1$ spatial eigenvalues include 0 (due to symmetries), $i\sqrt{\mu + n}$ for $k = n$, and

$$i\sqrt{\mu + s_k}, \quad k = 1, \ldots, n-1.$$

The frequency $\sqrt{\mu + n}$ produces the Vertical Lyapunov family, which corresponds to the oscillatory ring in Meyer and Schmidt (1993). For $k = n/2$, with n even, we obtain a Hip-Hop family Meyer and Schmidt (1993). For the Maxwell configuration, we say that a Lyapunov orbit is $\ell : m$ resonant when its period satisfies

$$T_{\ell:m} = \frac{2\pi}{\sqrt{\mu + s_1}} \frac{\ell}{m},$$

where ℓ and m are relatively prime such that $k\ell - m \in n\mathbb{Z}$. For an $\ell : m$ resonant Lyapunov orbit, the n bodies of equal mass follow the same path as in Theorem 1. From the many families and the many resonant orbits that we have determined, we show only a few Planar and spatial resonant orbits in Fig. 10, namely for $n = 7$, with $\mu = 200$, and for $n = 8$, with $\mu = 300$.

7.2 The Figure-Eight choreography

In this article, we have shown that pseudo-arclength continuation is a powerful tool for following periodic solutions of conservative systems, and with it the detection of resonant orbits, including choreographies. A basic assumption is the presence of a single eigenvalue in the kernel. The continuation of families of periodic solutions starting with frequencies $\sqrt{s_1}$ from Lagrange solutions of the 3-body problem represents a bifurcation problem with five eigenvalues in the kernel, i.e., multiple planar and spatial solutions bifurcate with frequency $\sqrt{s_1}$. In Chenciner and Féjoz (2009) and García-Azpeitia and Ize (2013), it is proved that a Vertical family of periodic solutions bifurcates from the Lagrange solution. Also, in Chenciner et al. (2005), it is proved that three families of periodic solutions bifurcate from the Figure-Eight choreography. It is also conjectured that one of them, the Marchal P12 family, connects to the Vertical family from the Lagrange solution. The proof of this conjecture remains open. In principle, higher multiplicity cases can also be dealt with by continuation, and we intend to do so in more generality in future work. However, here we do follow one of the families that arise from the Figure-Eight choreography, namely a Planar family that contains a dense set of resonant orbits that correspond to choreographies, as shown in Fig. 11. Some of these choreographies have been found in Chenciner et al. (2002) as subharmonic solutions of the Poincaré return map around the Figure-Eight choreography. Numerically, we find that these subharmonic solutions correspond to resonant orbits along a continuous family in rotating coordinates, which has been proved to exist in Chenciner et al. (2005). We find that the solutions along this Planar family have characteristic multipliers that are on the unit circle or very close to the unit circle, i.e., some of the choreographies along the family may be linearly

stable. Other continuations form the Figure-Eight choreography have been done in Doedel et al. (2002) by varing the masses.

Acknowledgements We thank R. Montgomery, J. Montaldi, D. Ayala, and L. García-Naranjo for many interesting discussions. We also acknowledge the assistance of Ramiro Chavez Tovar with the preparation of figures and animations. This research was also supported by NSERC (Canada) Grant N00138. R. C. was partially supported by PAPIIT Project IA102818.

References

Alexander, J., Yorke, J.: Global bifurcations of periodic orbits. Am. J. Math. **100**, 263–292 (1978)
Barrabés, E., Cors, J.M., Pinyol, C., Soler, J.: Hip-hop solutions of the 2*n*-body problem. Celest. Mech. Dyn. Astronom. **95**(1–4), 55–66 (2006)
Barutello, V., Terracini, S.: Action minimizing orbits in the *n*-body problem with simple choreography constraint. Nonlinearity **17**, 2015–2039 (2004)
Barutello, V., Ferrario, D., Terracini, S.: Symmetry groups of the planar 3-body problem and action-mimizing trajectories. Arch. Ration. Mech. Anal. **190**, 189–226 (2008)
Calleja, R., Doedel, E., García-Azpeitia, C.: Symmetry-breaking for a restricted *n*-body problem in the Maxwell-ring configuration. Eur. Phys. J. ST **225**, 2741–2750 (2016)
Chen, K.-C.: Binary decompositions for planar n-body problems and symmetric periodic solutions. Arch. Ration. Mech. Anal. **170**, 247–276 (2003)
Chenciner, A., Féjoz, J.: Unchained polygons and the *n*-body problem. Regul. Chaotic Dyn. **14**(1), 64–115 (2009)
Chenciner, A., Montgomery, R.: A remarkable periodic solution of the three-body problem in the case of equal masses. Ann. Math. **152**(2), 881–901 (2000)
Chenciner, A., Gerver, J., Montgomery, R., Simó, C.: Simple choreographic motions of N bodies A preliminary study. In: Marsden, J.E., Newton, P., Holmes, P., Weinstein, A. (eds.) Geometry, Mechanics, and Dynamics, 60th birthday of J. E. Marsden. Springer, New York (2002)
Chenciner, A., Féjoz, J., Montgomery, R.: Rotating eights I: the three Γ_i families. Nonlinearity **18**, 1407–1424 (2005)
Doedel, E., Freire, E., Galán, J., Muñoz-Almaraz, F., Vanderbauwhede, A.: Stability and bifurcations of the figure-8 solution of the three-body problem. Phys. Rev. Lett. **88**, 241101 (2002)
Ferrario, D.: Symmetry groups and non-planar collisionless action-minimizing solutions of the three-body problem in three-dimensional space. Arch. Ration. Mech. Anal. **179**(3), 389–412 (2006)
Ferrario, D., Portaluri, A.: On the dihedral *n*-body problem. Nonlinearity **21**(6), 1307–1321 (2008)
Ferrario, D., Terracini, S.: On the existence of collisionless equivariant minimizers for the classical *n*-body problem. Invent. Math. **155**(2), 305–362 (2004)
García-Azpeitia, C., Ize, J.: Global bifurcation of polygonal relative equilibria for masses, vortices and dNLS oscillators. J. Differ. Equ. **251**, 3202–3227 (2011)
García-Azpeitia, C., Ize, J.: Global bifurcation of planar and spatial periodic solutions in the restricted n-body problem. Celest. Mech. Dyn. Astron. **110**, 217–227 (2011)
García-Azpeitia, C., Ize, J.: Global bifurcation of planar and spatial periodic solutions from the polygonal relative equilibria for the *n*-body problem. J. Differ. Equ. **254**, 2033–2075 (2013)
Ize, J., Vignoli, A.: Equivariant Degree Theory. De Gruyter Series in Nonlinear Analysis and Applications 8. Walter de Gruyter, Berlin (2003)
Kapela, T., Simó, C.: Rigorous KAM results around arbitrary periodic orbits for Hamiltonian Systems. Preprint (2017)
Kapela, T., Simó, C.: Computer assisted proofs for nonsymmetric planar choreographies and for stability of the Eight. Nonlinearity **20**, 1241–1255 (2007)
Kapela, T., Zgliczynski, P.: An existence of simple choreographies for *N*-body problem: a computer assisted proof. Nonlinearity **16**, 1899–1918 (2003)
Marchal, C.: The family P12 of the three-body problem. The simplest family of periodic orbits with twelve symmetries per period. Celest. Mech. Dyn. Astron. **78**, 279–298 (2000)
Marchal, C.: How the method of minimization of action avoids singularities. Celest. Mech. Dyn. Astron. **83**, 325–353 (2002)
Meyer, K., Schmidt, D.: Librations of central configurations and braided saturn rings. Celest. Mech. Dyn. Astron. **55**(3), 289–303 (1993)
Moeckel, R.: Linear stability of relative equilibria with a dominant mass. J. Dyn. Differ. Equ. **6**, 37–51 (1994)

Montaldi, J., Steckles, K.: Classification of symmetry groups for planar n-body choreographies. Forum of Mathematics, Sigma 1 (2013)
Moore, C.: Braids in classical gravity. Phys. Rev. Lett. **70**, 3675–3679 (1993)
Muñoz-Almaraz, F., Freire, E., Galán, J., Doedel, E., Vanderbauwhede, A.: Continuation of periodic orbits in conservative and Hamiltonian systems. Phys. D **181**, 1–38 (2003)
Roberts, G.E.: Linear stability in the $1+n$-non relative equilibrium. In: Delgado, J. (ed), Hamiltonian Systems and Celestial Mechanics. HAMSYS-98. Proceedings of the 3rd International Symposium, World Sci. Monogr. Ser. Math. 6. World Scientific, pp. 303–330 (2000)
Simó, C.: New families of solutions in N-body problems. In: European Congress of Mathematics. Springer Nature, pp. 101–115 (2001)
Terracini, S., Venturelli, A.: Symmetric trajectories for the $2n$-body problem with equal masses. Arch. Ration. Mech. Anal. **184**(3), 465–493 (2007)
Vanderbei, R., Kolemen, E.: Linear stability of ring systems. Astron. J. **133**, 656–664 (2007)